Deep-Sea Research I 69 (2012) 70–81

Contents lists available at SciVerse ScienceDirect

Deep-Sea Research I

journal homepage: www.elsevier.com/locate/dsri

Primary production and bacterial carbon metabolism around South Shetland Islands in the Southern Ocean

Eva Teira [a,*], Beatriz Mouriño-Carballido [a], Sandra Martínez-García [a,1], Cristina Sobrino [a], Julia Ameneiro [a], Santiago Hernández-León [b], Elsa Vázquez [a]

[a] Departamento Ecoloxía e Bioloxía Animal, Facultade de Ciencias do Mar, Universidade de Vigo, 36200 Vigo, Spain
[b] Institute of Oceanography and Global Change, Universidad de Las Palmas de Gran Canaria, Spain

ARTICLE INFO

Article history:
Received 23 February 2012
Received in revised form
21 May 2012
Accepted 5 July 2012
Available online 17 July 2012

Keywords:
Primary production
Photochemical efficiency
Bacterial production
Bacterial growth efficiency
South Shetland Islands
Drake Passage

ABSTRACT

Phytoplankton and bacterioplankton dynamics were studied around South Shetland Islands (Antarctica) with special emphasis on the Drake Passage region, during austral summer, in order to expand our knowledge on the coupling between the autotrophic and heterotrophic microbial plankton compartments in polar ecosystems. In addition, we directly estimated bacterial growth efficiency in the Drake Passage with the aim of better constraining total bacterial carbon utilization in this important polar ecosystem. Integrated chlorophyll-a concentration (21–86 mg m^{-2}), primary production rates (0.7–19.3 mg C m^{-3} d^{-1}) and mean water-column photochemical efficiency (0.24–0.60) were significantly correlated with Si* tracer ($r^2=0.55$, 0.46 and 0.64, respectively), which indirectly points to iron as the major limiting factor for phytoplankton growth in the area. Bacterial production was considerably low (0.002–0.3 mg C m^{-3} d^{-1}) and was best explained by chlorophyll-a concentration, protein-like fluorescence of dissolved organic matter and temperature ($r^2=0.53$, $p<0.001$). Water temperature appeared to influence bacterial activity when organic substrate availability is high. Bacterial production accounted on average for only 3.9% of co-occurring primary production, which has been frequently interpreted as an indicator of the marked uncoupling between bacteria and phytoplankton in cold waters. However, using the experimentally derived mean bacterial growth efficiency for the photic zone ($6.1\pm1.3\%$) the bacterial carbon demand represented on average $63\pm18\%$ of concomitant primary production, similar to what is found in warmer productive waters. Thus, our study suggests that bacterioplankton and phytoplankton appear to be connected in this polar area.

1. Introduction

The Southern Ocean represents 20% of the global ocean and is a critical sink for excess atmospheric carbon (Sarmiento and Le Quéré, 1996). The annual mean temperature in the Antarctic Peninsula (AP) region has increased 2 °C since 1950, which has translated into a rapid warming of shelf waters west of AP by 0.6 °C (Ducklow et al., 2007). Such rapid changes may lead to higher microbial plankton activity and less energy and organic carbon for supporting higher trophic levels (Kirchman et al., 2009).

The area around South Shetland Islands (SSI) off the northern tip of the Antarctic Peninsula sustains elevated phytoplankton biomass during the austral summer, while high nutrient-low chlorophyll (HNLC) conditions prevail in Drake Passage to the north and in the Bransfield Strait to the south (Hewes, 2009). The Drake Passage Antarctic Surface Water (ASW) mass to the north of the SSI develops a warm and less saline upper mixed layer during the austral summer where phytoplankton growth is limited by low iron concentration (Holm-Hansen and Hewes, 2004). On the other hand, intense mixing of iron-replete Transitional Weddell Water (TWW) appears to cause phytoplankton light limitation in the south of Bransfield Strait (Hewes et al., 2008).

Bacterial consumption of dissolved organic matter represents a critical trophic link that supports higher trophic levels and nutrient regeneration in the ocean (Azam, 1998). Primary production is the ultimate source of most organic material in the sea, and it is estimated that about 50% of primary production is consumed by heterotrophic bacteria in low latitude oceans (Robinson, 2008). By contrast, a much lower percentage of primary production is utilized by bacteria in polar systems (Bird and Karl, 1999; Ducklow, 2000; Morán et al., 2001; Kirchman et al., 2009; Ducklow et al., 2012) which has been considered as indicative of phytoplankton–bacteria uncoupling (Billen and Becquevort, 1991; Karl, 1993). Such low bacterial activity has been ascribed to temperature limitation (Pomeroy and Deibel, 1986), limited dissolved organic matter (DOM) availability (Bird and Karl, 1999), a combination of temperature and DOM regulation (Pomeroy and Wiebe, 2001), or a strong grazing pressure

* Corresponding author. Tel.: +34 986 812591; fax: +34 986 812556.
E-mail address: teira@uvigo.es (E. Teira).
[1] Present address: Department of Oceanography, University of Hawaii, Honolulu, 96822 HI, USA

0967-0637/$ - see front matter © 2012 Elsevier Ltd. All rights reserved.
http://dx.doi.org/10.1016/j.dsr.2012.07.002

(Bird and Karl, 1999; Duarte et al., 2005). However, growing evidence points to questionable higher grazing control in polar waters than elsewhere and to negligible effect of low temperature on bacterial growth in polar oceans (Ducklow et al., 2001, 2012; Kirchman et al., 2009). Therefore, the bacterial metabolism in these perennially cold waters seems to be essentially limited by dissolved organic matter availability.

Although several studies have described phytoplankton biomass distribution around or nearby SSI (Basterretxea and Arístegui, 1999; Kelley et al., 1999; Kawaguchi et al., 2001; Varela et al., 2002; Holm-Hansen and Hewes, 2004; Hewes et al., 2008), only a few have measured primary production rates and/or phytoplankton physiological parameters (Burkholder and Mandelli, 1965; Basterretxea and Arístegui, 1999; Kelley et al., 1999; Lorenzo et al., 2002). On the other hand, there are only a few reports of bacterial production (BP) rates around or nearby SSI (Karl et al., 1991; Kelley et al., 1999; Morán et al., 2001; Pedrós-Alió et al., 2002; Ortega-Retuerta et al., 2008; Manganelli et al., 2009), and to the best of our knowledge none simultaneously reporting BP and bacterial respiration (BR) rates. Only a few papers have directly or indirectly assessed the degree of phytoplankton–bacterioplankton coupling in the region (Mullins and Priddle, 1987; Kelley et al., 1999; Karl et al., 1991; Morán et al., 2001; Ortega-Retuerta et al., 2008), although they do not include much data on autotrophic and heterotrophic microbial plankton production rates in the Drake Passage. Some of the most recent studies in the vicinity of Bransfield strait have concluded a relatively close coupling between phytoplankton and bacteria (Morán et al., 2001; Ortega-Retuerta et al., 2008).

The main objective of our study was to expand our knowledge on phytoplankton and bacterioplankton dynamics and their couplings around SSI, with special emphasis on the Drake Passage region. In addition, we directly estimated bacterial growth efficiency at 3 different stations in the Drake Passage in order to better constrain total bacterial carbon utilization in this important polar ecosystem. As far as we know, these are the first direct estimations of bacterial respiration in the area.

2. Materials and methods

2.1. Study area and sampling

Sampling was carried out during the COUPLING cruise in January 2010 on board the RV Hespérides along 7 transects around the SSI (Fig. 1). At each station vertical profiles of temperature, salinity and in situ fluorescence were obtained using a Conductivity–Temperature–Depth sensor (CTD) Seabird 911plus attached to the rosette, down to the bottom in the coastal and the shelf stations and down to 1000 m in the offshore stations. The depth of the upper mixed layer (UML) was computed as the depth where potential density differed by 0.05 Kg m^{-3} from the mean potential density measured at the surface (Mitchell and Holm-Hansen, 1991). Photosynthetically active radiation (PAR, 400–700 nm) was measured with a Satlantic OCP-100FF radiometer attached to the rosette.

Samples for nutrients and plankton-related variables (size-fractionated chlorophyll-a concentration, dissolved organic matter (DOM) fluorescence and bacterial production) were collected at 5–6 depths (between 5 and 150 m) using 12 l acid-clean Niskin bottles attached to a rosette sampler. Bacterial production rates and DOM fluorescence were measured at 2–3 additional depths (from 200 to 480 m depth) along transect TB (Fig. 1). Primary production was measured at 11 selected stations (station 5, 8, 10, 26, 29, 33, 36, 42, 61, 68, 76) in surface waters and at the deep chlorophyll maximum (DCM) depth.

2.2. Size-fractionated chlorophyll-a concentration

Chlorophyll-a (chla) concentration was determined fluorometrically. 250-mL water samples were sequentially filtered through 0.2, 2 and 20 μm polycarbonate filters and pigments were extracted in 90% acetone at −20 °C overnight. Fluorescence was measured on a Turner TD-700 fluorometer which had been calibrated with pure chlorophyll a.

2.3. Fluorescence of dissolved organic matter

Samples for fluorescence of dissolved organic matter (FDOM) determination were collected into 200 mL acid-cleaned borosilicate bottles and filtered by hand with 100 ml polyethylene syringes with teflon plunger tips through Whatman Puradisc GF/F disposable filter devices (0.45 μm pore size) on polypropylene housing. The filtering system and syringes were previously "washed" with 0.1 N HCl and rinsed with Mili-Q water. In addition, the syringes were rinsed three times with sample. FDOM was measured with a Perkin Elmer LS 55 luminescence spectrometer equipped with a xenon discharge lamp, equivalent to 20 kW for 8 μs duration. Measurements were performed in a 1 cm quartz fluorescence cell.

Discrete excitation/emission (E_x/E_m) pair measurements were performed at peak-T, characteristic of protein-like substances

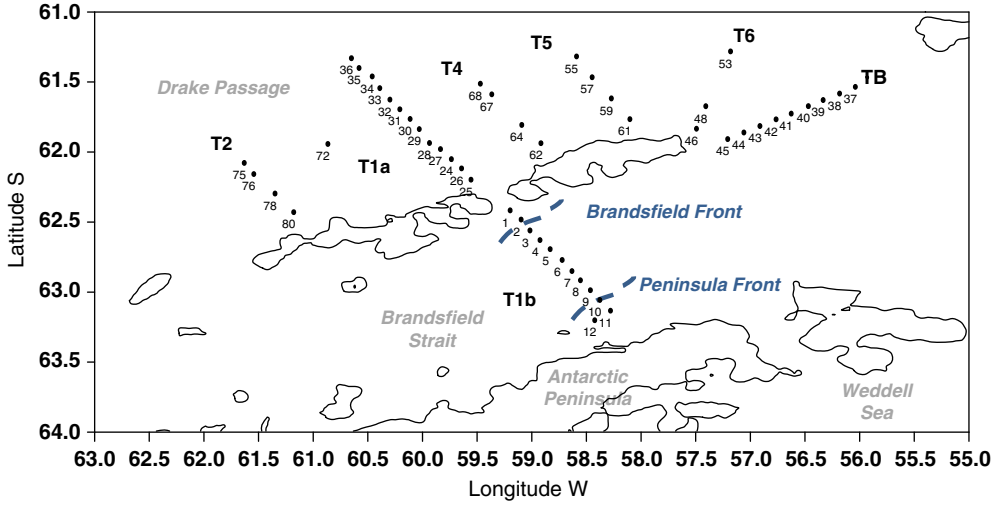

Fig. 1. Map showing stations sampled around the South Shetland Islands (SSI) during the COUPLING cruise. Numbers indicate CTD stations.

(E_x/E_m: 280 nm/350 nm). Four replicate measurements were performed for each E_x/E_m pair. The system was calibrated with a mixed standard of quinine sulfate (QS) and tryptophan (Trp) in sulfuric acid 0.05 M (Nieto-Cid et al., 2005). The equivalent concentration of every peak was determined by subtracting the average peak height from the corresponding milli-Q water blank height and dividing by the slope of the standard curve. Fluorescence units were expressed in ppb equivalents of Trp (ppb Trp). The precision was ± 0.6 ppb Trp.

2.4. Nutrients

Aliquots for inorganic nutrients determination (ammonium, nitrite, nitrate, phosphate and silicate) were collected in 10 ml polyethylene tubes and frozen at $-80\,^{\circ}C$ until analysis by standard colorimetric methods with a Technicon TRAACS 800 analyzer (Hansen and Grasshoff, 1983).

We used the Si* tracer (calculated as the concentration of silicate minus nitrate concentration) defined by Sarmiento et al. (2003) as a proxy for iron limitation in the sampling area. The Si* is as high as 50 $\mu mol\,l^{-1}$ to the south of the polar front, where upwelling injects nutrient-rich water to the surface of the Southern Ocean. The Si* reach values of zero or negative in the Polar Front, near 61°S, as a consequence of the preferential removal of silicic acid over nitrate by diatoms associated to iron limitation (Sarmiento et al., 2003).

2.5. Primary production

Primary production was measured using the ^{13}C method (Hama et al., 1983) in a total of 11 stations at two sampling depths, including surface ($\sim$5 m depth) and at the depth of the deep chlorophyll maximum (DCM). Water samples were transferred to 2 L polycarbonate bottles previously rinsed with 10% HCl and distilled-deionized water. After addition of $NaH^{13}CO_3$ at about 10% of total inorganic carbon in the ambient water, the samples were incubated for about 12 h in a tank on deck at in situ temperature with running surface seawater under light intensity regulated by meshes of different sizes to simulate in situ conditions. Initial and final particulate organic carbon, and particulate material used for isotope analysis were filtered through GF/F filters. They were frozen and stored at $-20\,^{\circ}C$ until analysis. POC was measured using a CHN analyzer (Carlo Erba EA 1108) and isotopes in a mass spectrometer equipped with an elemental analyzer (Flash EA11 ThermoFinnigan with Deltaplus).

2.6. Photochemical efficiency (F_v/F_m)

Fast Repetition Rate fluorometer (FRRf) data was acquired using a FASTracka I instrument from Chelsea Instruments down to 50–110 m depth. Saturating-chain sequences of 100 1.1 μs flashes were applied at 2.8 μs intervals. Fluorescence transients were logged internally during profiling from the average of 16 successive sequences. Data were alternately acquired from the open ("light") and enclosed ("dark") chambers every 100 ms. In contrast with usual practice, the FRRf was not deployed on the CTD/cage+rosette, but by itself on a winch cable through the starboard side of the ship. For most of the casts shown in this paper, data were combined from 2 to 3 sequential vertical ascents. Profiles were recorded starting from below the mixed layer at 10 m min^{-1}. The slow ascent rate and high number of profiles were carried out to ensure adequate coverage, especially in the photoactive zone, which is characterized by strong vertical gradients in irradiance and fluorescence. A typical profile series took 30–45 min to perform. All data were processed using FRS software (Chelsea Technologies Ltd.) correcting for instrument response function and seawater blank. The latter was obtained by filtering water from each station by 0.2 μm pore filters. Values shown in the paper correspond to those acquired with the dark chamber in order to calculate dark-adapted maximum quantum efficiency, $F_v/F_m=(F_m-F_0)/F_m$, being F_0 and F_m the minimum fluorescence rate and the maximum fluorescence rate after the saturating-chain sequences, respectively, when all the reaction centers are closed. For more information regarding profiling and data processing see Neale et al. (2012).

2.7. Bacterial production

Bacterial production was measured with the [^{3}H]-Leucine (Leu) uptake method (Smith and Azam 1992). Samples were incubated in the dark at in situ temperature using temperature-controlled water baths. For each sampling depth three aliquots (1 ml) plus two trochloroacetic acid-killed controls were placed into eppendorf tubes and incubated with Leu at saturating concentration (40 nmol l^{-1} final concentration) for 2–5 h. Mean DPMs in the killed-controls were averaged 87 dpm (n=257). The variation coefficient of triplicate leucine assays was 17%. The detection limit (DL) for leucine incorporation rates (DL=mean blank+3 standard deviation) was 1.4 pmol Leu L^{-1} h^{-1} for a 2 h incubation. The Leu concentration was tested for rate saturation in the sampling zone at the beginning of the cruise. Empirical Leu-to-carbon conversion factors (CFs) were determined at station 10, at 5 and 50 m depths, following the methods detailed elsewhere (Calvo-Díaz and Morán, 2009). The CFs were estimated using the cumulative method (Bjørnsen and Kuparinen., 1991). As no significant differences were found between 5 and 50 m, the mean CF (0.74 ± 0.18 Kg C mol Leu^{-1}) was used to calculate bacterial biomass production rates from Leu uptake rates.

2.8. Bacterial respiration

Bacterial respiration rates were measured with the O_2 consumption method at two different depths (surface mixed layer and 100 m) at stations 64, 72 and 78. Eight 1.2 μm-filtered water samples were collected from each depth through silicon tubing into dark, calibrated borosilicate glass bottles with a nominal volume of 120 mL. Four bottles were incubated in the dark at in situ temperature for 72 h in the same water baths used for BP estimations. The other four samples were fixed immediately to determine the initial oxygen concentrations. Measurements of dissolved oxygen were made with an automated Winkler titration system using a potentiometric end-point detector. Detailed methods and error quantification are described elsewhere (Mourino-Carballido and McGillicuddy, 2006). A respiratory quotient (RQ) of 0.8 (Williams and del Giorgio, 2005) was used. Bacterial growth efficiency (BGE) was calculated as follows: bacterial production/(bacterial production+bacterial respiration).

3. Results

3.1. Hydrography

Based on the previous studies (García et al., 1994; Holm-Hansen et al., 1994; Sangrá et al., 2011) and on hydrographic data collected during COUPLING cruise we identified different water masses at the sampling stations, as defined by their temperature and salinity characteristics (Fig. 2). The water masses found in the northern Drake Passage area (T1a, T2, T4, T5 and T6, see Fig. 1) comprise the relatively warm and fresh Antarctic Surface Water (ASW) in the upper mixed layer (10–50 m depth), the colder and saltier Winter Water (WW) between 60 and 100 m depth, and, below the WW, in the northernmost stations, the relatively warm

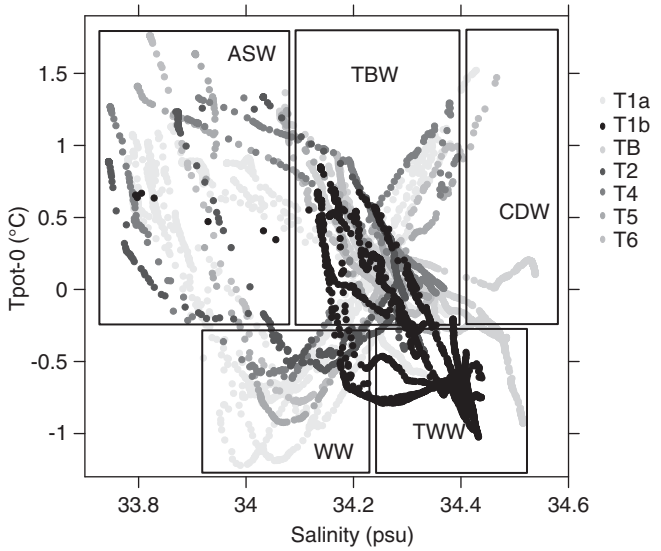

Fig. 2. T–S diagram of the sampling points showing the different water masses: Antarctic Surface Water (ASW), Winter Water (WW), Transitional Zonal Water with Bellingshausen influence (TBW), Circumpolar Deep Water (CDW), Transitional Weddell Water (TWW).

and salty Circumpolar Deep Water (CDW). In the southern part of transects T1a, T2, T4, T5 and T6, the Transitional Zonal Water with Bellingshausen influence (TBW) is located over the shelf. The water masses found in the Bransfield Strait (T1b) essentially include the TBW, at the most northerly stations, and the colder (Fig. 3A) and saltier Transitional Weddell Water (TWW) in the southern stations (stations 11–12), separated by a hydrographic front, known as the Peninsular Front (PF), located between stations 9 and 10 (Fig. 1). A slope front, the so-called Bransfield Front (BF), is located along the southern SSI between stations 1 and 3. Transect TB shows hydrographic characteristics similar to T1b (essentially TBW and TWW). A detailed description of the water masses, fronts, and circulation in the Brandsfield Strait is described elsewhere (Sangrá et al., 2011).

The integrated water column Si* in the northern Drake Passage area is lower than at southern latitudes (Fig. 3B), presumably as a consequence of iron limitation.

3.2. Chlorophyll-a concentration

The vertical distribution of total chlorophyll-a (chla) concentration along the sampled transects was tightly coupled to hydrography (Fig. 4). Chlorophyll-a concentration was very low (<0.4 mg chla m^{-3}) in the upper mixed layer (down to 50 m) in the northern part of T1a, T2, T4, T5 and T6, corresponding to the ASW (sigma-t <27.25 Kg m^{-3}). A Deep Chlorophyll Maximum (DCM) developed at these stations associated to the relatively cold WW (sigma-t 27.25–27.4 Kg m^{-3}), between 60 and 80 m depth. Higher chla concentration (>0.9 mg chla m^{-3}) was found in the upper mixed layer in the southern part of these transects and in TB. The highest chla concentrations (>1.8 mg chla m^{-3}) were found in the upper mixed layer in the southern part of T1b, associated to the hydrographic front (station 9). Chla concentration was homogeneously high (>0.8 mg chla m^{-3}) in the upper 90 m at stations 11 and 12, associated to the TWW (sigma-t >27.65 Kg m^{-3}). On average, the pico-(<2 μm) and nano-(<20 μm) size fractions represented 84% of total chlorophyll-a concentration in the sampling area (data not shown). Microphytoplankton (>20 μm) was relatively important (>30%) only close to the coast in transects T1a and T1b (Fig. 5). The contribution of large phytoplankton also slightly increased towards the north in the Drake Passage area.

Integrated total chla concentration ranged from <25 mg chla m^{-2} in the northern part of Drake Passage (stations 75, 30–36, 67, 55, 57 and 53) to >80 mg chla m^{-2} associated to the hydrographic front in the Bransfield Strait (stations 8–10) (Fig. 6A). Low integrated chla concentration (<40 mg m^{-2}) was also measured at stations 3 and 4 in the Bransfield Strait. Integrated chla concentration was positively related with integrated Si* ($r^2=0.55$, $p<0.01$, $n=42$), and not significantly related to the upper mixed layer (UML depth) ($p>0.05$, $n=47$).

3.3. Photochemical efficiency (F_v/F_m)

FRRF profiles were conducted in a total of 39 stations at different day times and under contrasting levels of PAR. We detected strong photoinhibition (operationally defined as a >50% reduction in surface F_v/F_m values compared to the subsurface mean values) in 5 out of 39 vertical FRRF profiles (data not shown). In order to compare the mean water column F_v/F_m values among stations we excluded those values strongly affected by photoinhibition. The mean F_v/F_m values (down to 100 m depth) widely varied in the sampling area from 0.25 at station 36 in the northern Drake Passage area to 0.59–0.61 at stations 61, 62 and 64 in the northern shelf of SSI (Fig. 3C). The spatial distribution of the mean F_v/F_m over the sampling areas closely resembles that of integrated Si* (Fig. 3B) that explained 64% of the variability of mean photochemical efficiency ($r^2=0.64$, $p<0.01$, $n=36$). Changes in mean F_v/F_m were significantly correlated to increases in mean background relative fluorescence (F_0/chla) ($r^2=0.63$, $p<0.01$, $n=39$).

3.4. Primary production

Daily primary production rates ranged from 0.7 to 19.3 mg C m^{-3} d^{-1} (0.04–0.91 mg C m^{-3} h^{-1}) and were not significantly different in surface waters than at the DCM (*T*-test, $p>0.05$) (Table 1). The highest rates (>16 mg C m^{-3} d^{-1}) were measured at station 10, both at the surface and at the DCM. Primary production was low (<5 mg C m^{-3} d^{-1}) in surface waters at stations located in the northern part of the Drake Passage area (stations 29, 33, 36, 68 and 76), associated to low Si* (Fig. 3B). Primary production rates were positively correlated with chla concentration ($r^2=0.33$, $p=0.016$, $n=17$) and Si* ($r^2=0.46$, $p=0.001$, $n=22$). The corresponding assimilation numbers ranged from 0.06 (station 8) to 1.1 mg C (station 10) (mg chla)$^{-1}$ h^{-1}. On the other hand, the water column mean PP rates were positively correlated with the upper mixed layer depth (UML) ($r^2=0.38$, $p=0.024$, $n=11$).

3.5. Fluorescence of dissolved organic matter

The protein-like fluorescence of dissolved organic matter (FDOM-T) generally decreased with depth (Fig. 7). FDOM-T levels were comparatively higher in T1b than in the other transects, with surface values ranging from 7 to 13 ppb trp. The lowest surface values (<4 ppb Trp) were measured at the northern part of T1a, T5 and T2. Subsurface maximum FDOM-T levels were measured at stations 36 and 28.

3.6. Bacterioplankton metabolism

Bacterial production (BP) rates were generally low (<0.3 mg C m^{-3} d^{-1}) and coupled to hydrography (Fig. 8). Higher BP rates were measured in T1b, T2 and T4 than in the other sampled transects. The lowest BP rates throughout the upper water column (down to 150 m depth) (<0.07 mg C m^{-3} d^{-1}) occurred at the stations located in the northern part of the Drake Passage, whereas the highest rates (>0.2 mg C m^{-3} d^{-1}) were measured at stations 6, 7, 8, 64 and 80 in the upper mixed layer and at station 1 in the

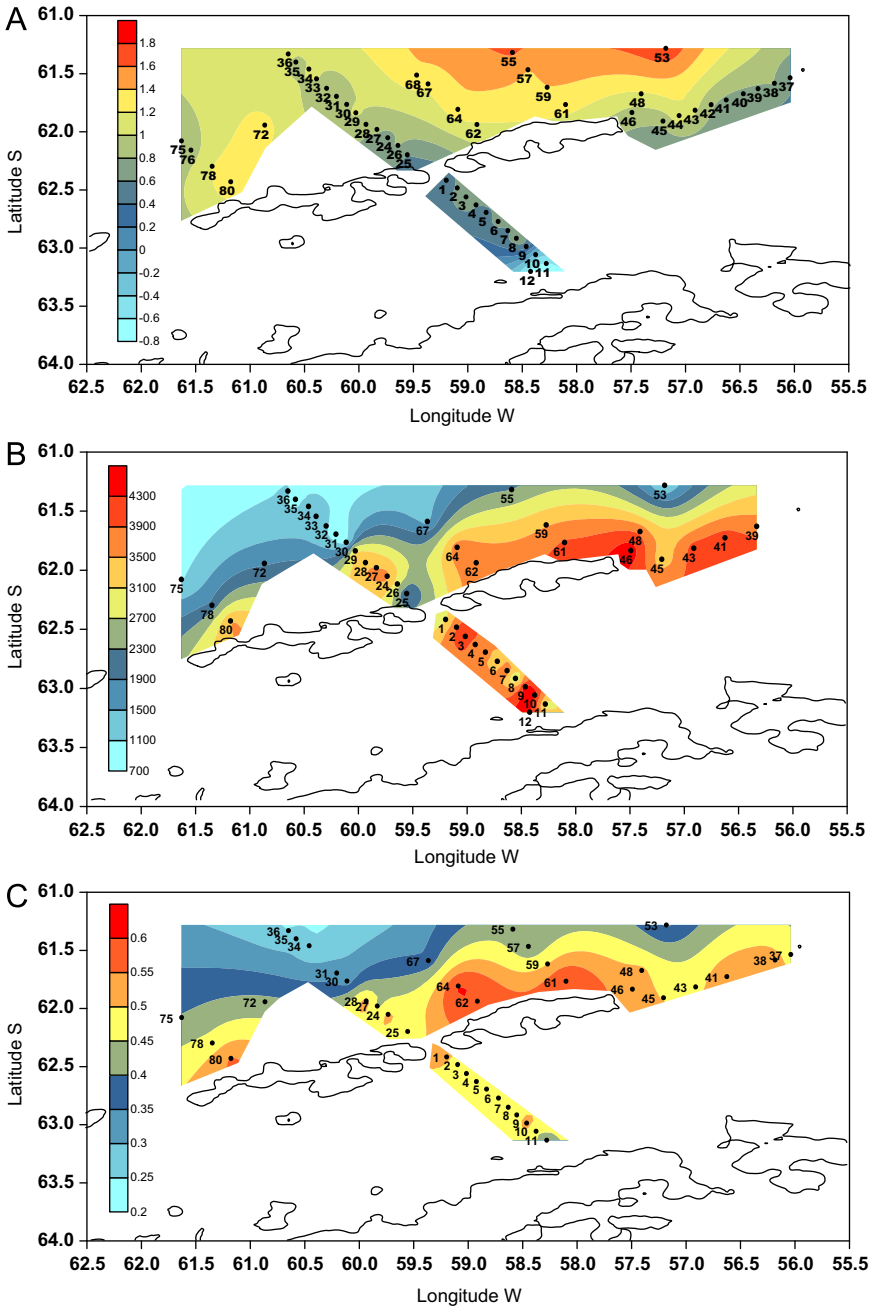

Fig. 3. Distribution of surface seawater temperature (°C) (A), integrated Si* tracer (mmol m^{-2}) (B), and mean F_v/F_m (C) in the sampling area. Data integrated or averaged down to 50 m for station 25, down to 75 m for stations 12 and 26, or down to 100 m. Numbers indicate CTD stations.

subsurface waters (75–100 m depth). BP was low (<0.035 mg C m^{-3} d^{-1}) and homogeneously distributed below 150 m in transect TB.

Integrated BP was generally low (<8 mg C m^{-2} d^{-1}) and maximum values (>14.2 mg C m^{-2} d^{-1}) were found at stations 1 and 64, located in the shelf of SSI (Fig. 6B). Lowest values were measured in the northern part of Drake Passage. Integrated BP was significantly and positively correlated with integrated chla concentration ($r^2=0.42$, $p<0.001$, $n=42$).

BP was significantly and positively correlated with temperature, ammonium, chla concentration and FDOM-T, and negatively with nitrate and phosphate concentration (Table 2). Multiple regression analysis showed that chla (beta coefficient=0.55, $p<0.001$), FDOM-T (beta coefficient=0.152, $p=0.007$) and temperature (beta coefficient=0.23, $p<0.001$) significantly contributed to explain 53% of the variability observed in the BP rates (adjusted $r^2=0.53$, $p<0.001$, $n=192$). In order to remove the effect of depth-related variability we repeated the multiple regression analysis using depth-integrated data (depth-averaged data for temperature), and we similarly found that chla (beta coefficient=0.47, $p=0.002$), FDOM-T (beta coefficient=0.33, $p=0.034$) and temperature (beta coefficient=0.31, $p=0.02$) significantly contributed to explain 47% of the variability observed in the BP rates (adjusted $r^2=0.47$, $p<0.001$, $n=42$). Primary production rates marginally correlated with the BP rates ($r^2=0.27$, $p=0.046$, $n=15$).

The role of temperature in modulating the BP rates is exemplified in Fig. 9. Both chla concentration and FDOM-T explained a higher percentage of variability in the BP rates at temperatures above 0 °C (slope=0.67, $r^2=0.46$, $p<0.001$, $n=124$ for chla; slope=0.27, $r^2=0.33$, $p<0.001$, $n=154$ for FDOM-T) than at

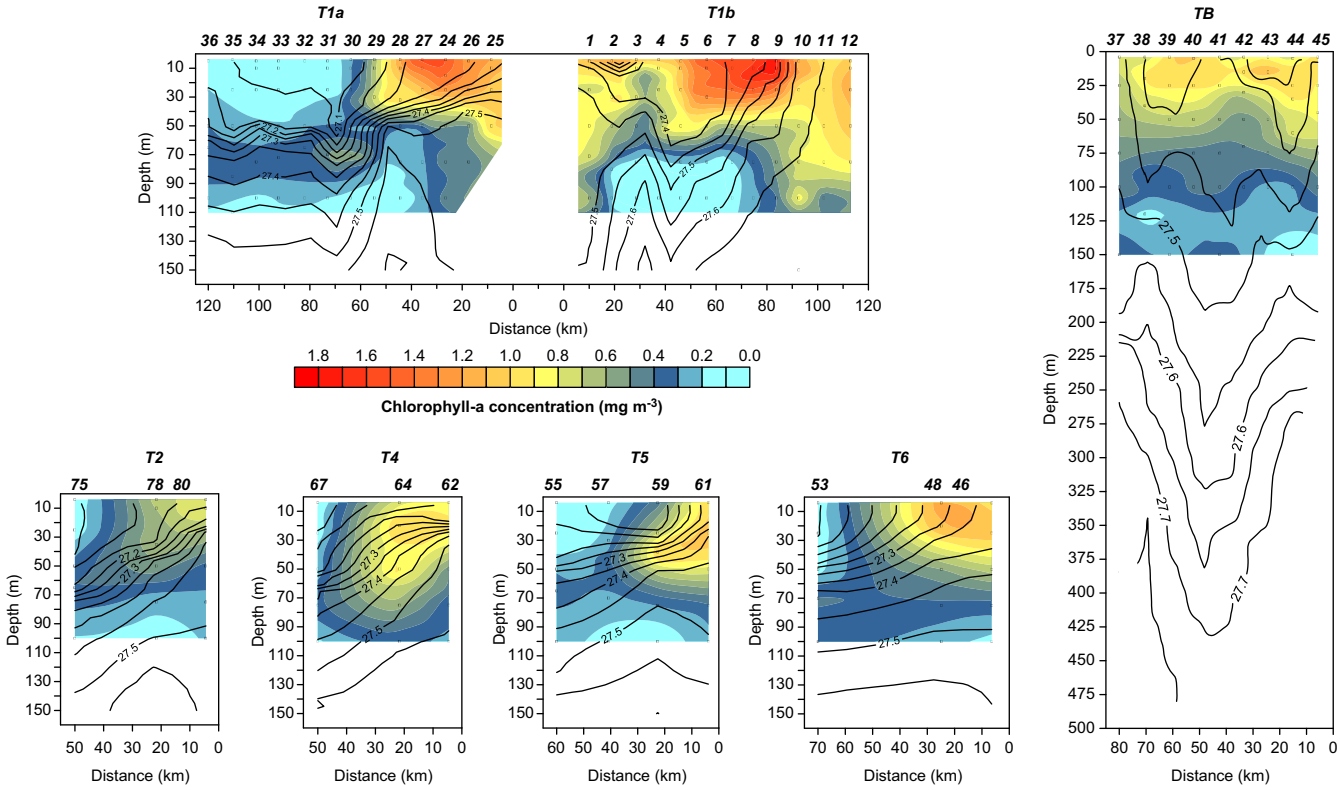

Fig. 4. Vertical distribution of total chlorophyll-a concentration (mg m^{-3}) along the transects sampled during the COUPLING cruise. Black superimposed isolines represent sigma-t. Numbers in the upper *X*-axis represent the station numbers.

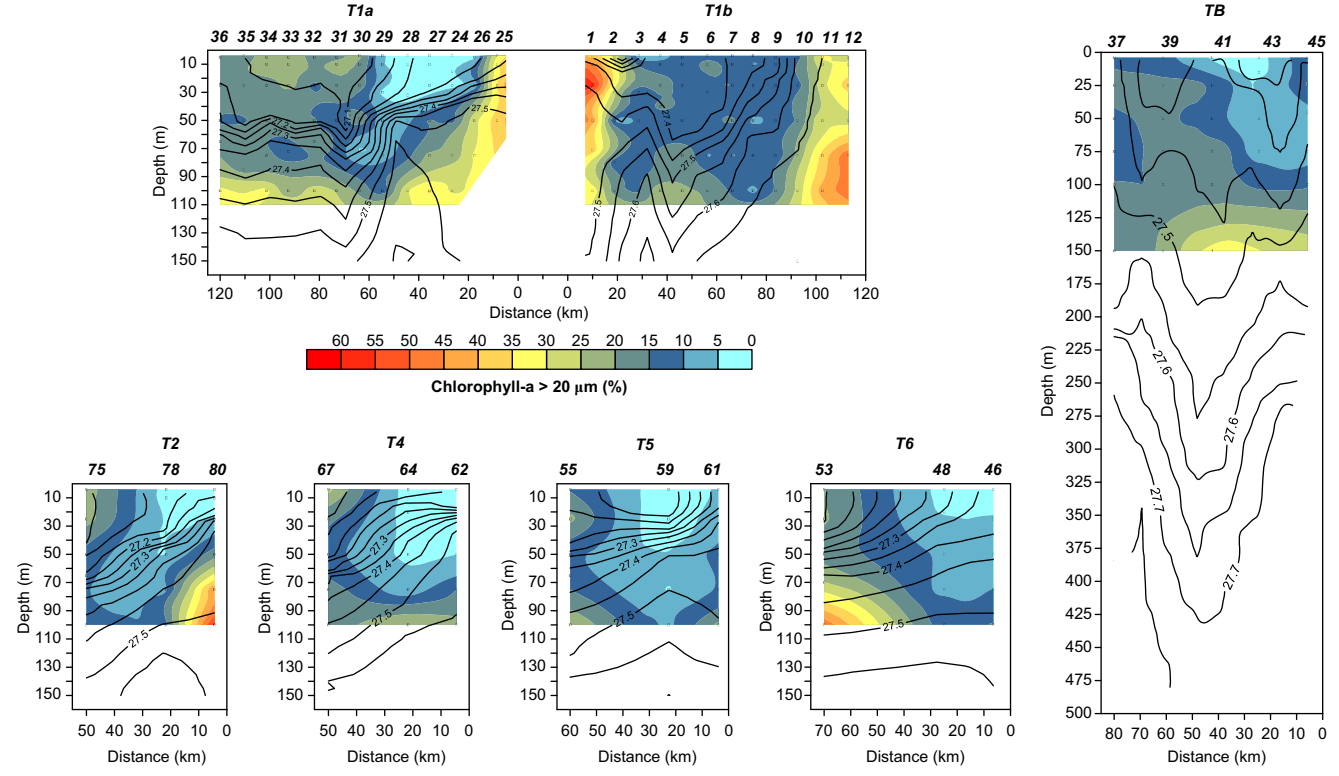

Fig. 5. Vertical distribution of the relative contribution of >20 µm phytoplankton to total chlorophyll-a concentration (%) along the transects sampled during the COUPLING cruise. Black superimposed isolines represent sigma-t. Numbers in the upper *X*-axis represent the station numbers.

temperatures below 0 °C (slope=0.49, r^2=0.31, $p<0.001$, n=71 for chla; $p>0.05$, n=85 for FDOM-T). Moreover, whereas the *y*-intercepts of the two chla-BP regression lines (Fig. 9A) were not significantly different (ANCOVA F-test, p=0.546), the slope of the regression line for the temperatures above 0 °C was significantly higher than the one derived for the temperatures below 0 °C

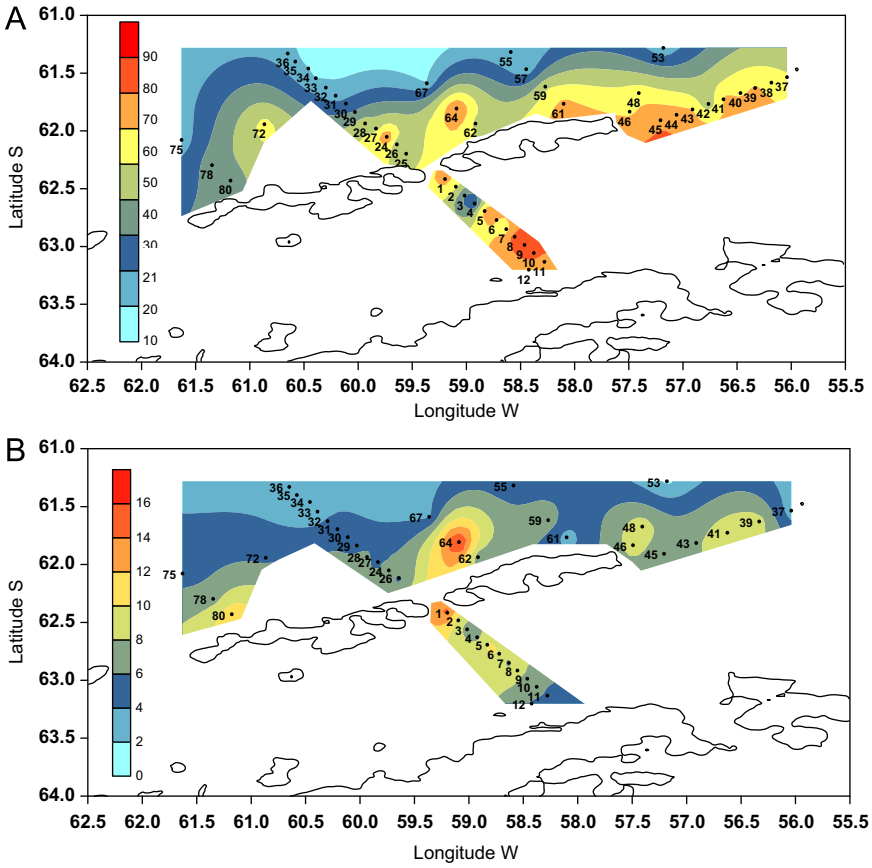

Fig. 6. Distribution of integrated chlorophyll-a concentration (mg m^{-2}) (A), and integrated bacterial production rates (mg C m^{-2} d^{-1}) (B) in the sampling area. Data integrated down to 50 m for station 25, down to 75 m for stations 12 and 26, or down to 100 m. Numbers indicate CTD stations.

Table 1
Sampling depth, rates of primary production (mg C m^{-3} d^{-1}) and chlorophyll-a concentration in surface waters and at the deep chlorophyll maximum (DCM) at selected stations. ND, not determined.

Station number	Surface			DCM		
	Depth (m)	PP (mg C m^{-3} d^{-1})	Chla (mg m^{-3})	Depth (m)	PP (mg C m^{-3} d^{-1})	Chla (mg m^{-3})
5	4	6.36	1.17	50	5.87	1.16
8	4	6.51	1.48	26	1.92	1.58
10	5	19.32	1.15	48	16.69	0.72
26	4	13.22	1.22	10	9.52	ND
29	4	4.64	0.59	30	0.64	0.87
33	5	1.11	0.15	72	0.68	0.35
36	5	0.69	0.19	65	0.68	0.34
42	4	6.83	0.36	31	6.38	0.61
61	4	6.84	1.1	25	4.13	1.17
68	6	0.58	ND	60	2.34	ND
76	4	1.14	ND	76	1.01	ND

(ANCOVA F-test, $p=0.048$), which means that for the same chla value, the BP rates were overall higher above 0 °C than below 0 °C (Fig. 9A).

Bacterial respiration rates narrowly varied between 2.76 and 5.76 mg C m^{-3} d^{-1}, whereas the corresponding BP rates varied by one order of magnitude (from 0.024 to 0.504 mg C m^{-3} d^{-1}) (Table 3). The estimated bacterial growth efficiency (BGE) also varied by one order of magnitude from 0.6% at 100 m depth to 8% at 35 m depth at station 78. BGE was always higher in the upper mixed layer than at 100 m depth. BGE was significantly correlated with the chla concentration ($r^2=0.46$, $p<0.05$, $n=6$), FDOM-T ($r^2=0.71$, $p<0.01$, $n=5$) and temperature ($r^2=0.42$, $p<0.05$, $n=6$).

4. Discussion

4.1. Phytoplankton distribution, primary production and physiology

Phytoplankton biomass distribution, as reflected by chla distribution, was closely associated to hydrography (Fig. 4) as previously described in the region (Mullins and Priddle, 1987; Basterretxea and Arístegui, 1999; Hewes et al., 2009). Chlorophyll-a concentration, mostly due to pico- and nano-size cells, was within the range of previous measurements in the region (Burkholder and Sieburth, 1961; Mullins and Priddle, 1987; Kawaguchi et al., 2001; Varela et al., 2002; Holm-Hansen and

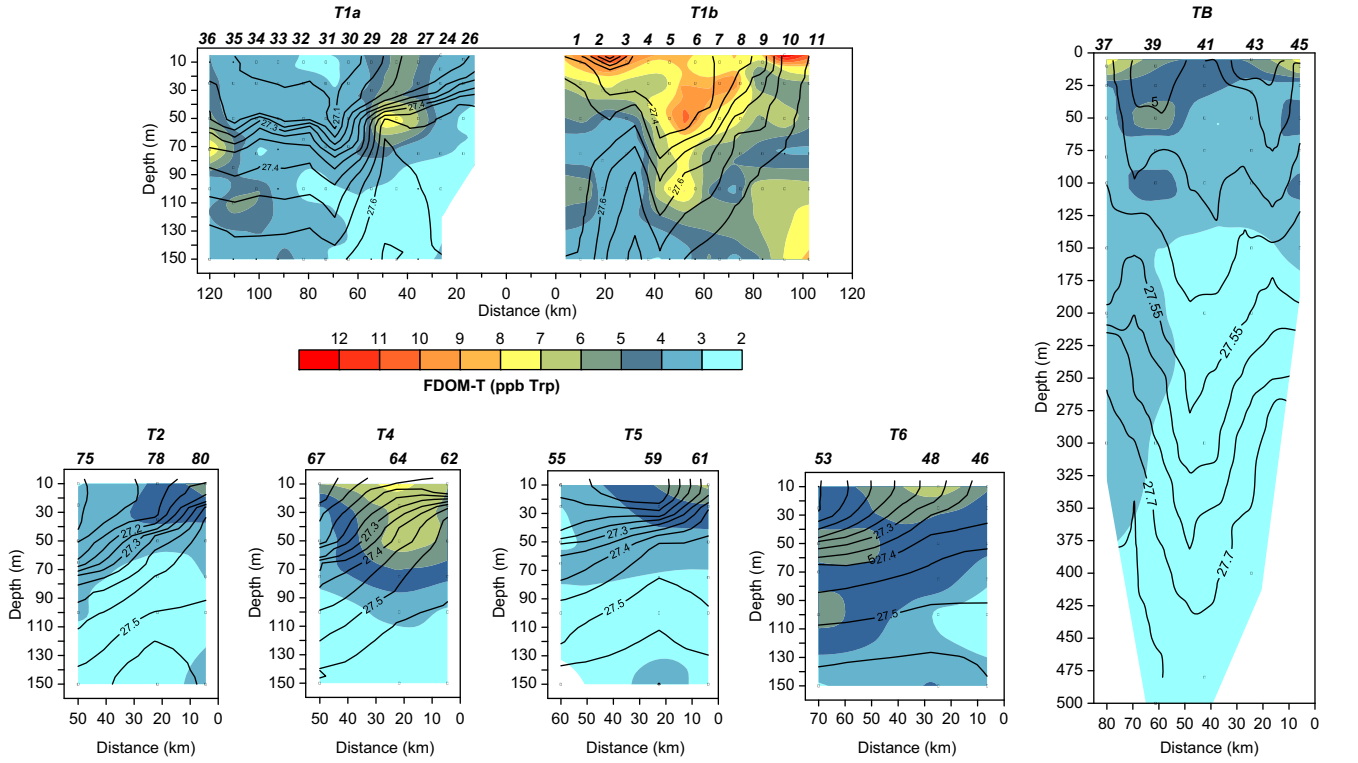

Fig. 7. Vertical distribution of protein-like fluorescence of dissolved organic matter (FDOM-T) (ppb Trp) along the transects sampled during the COUPLING cruise. Black superimposed isolines represent sigma-t. Numbers in the upper *X*-axis represent the station numbers.

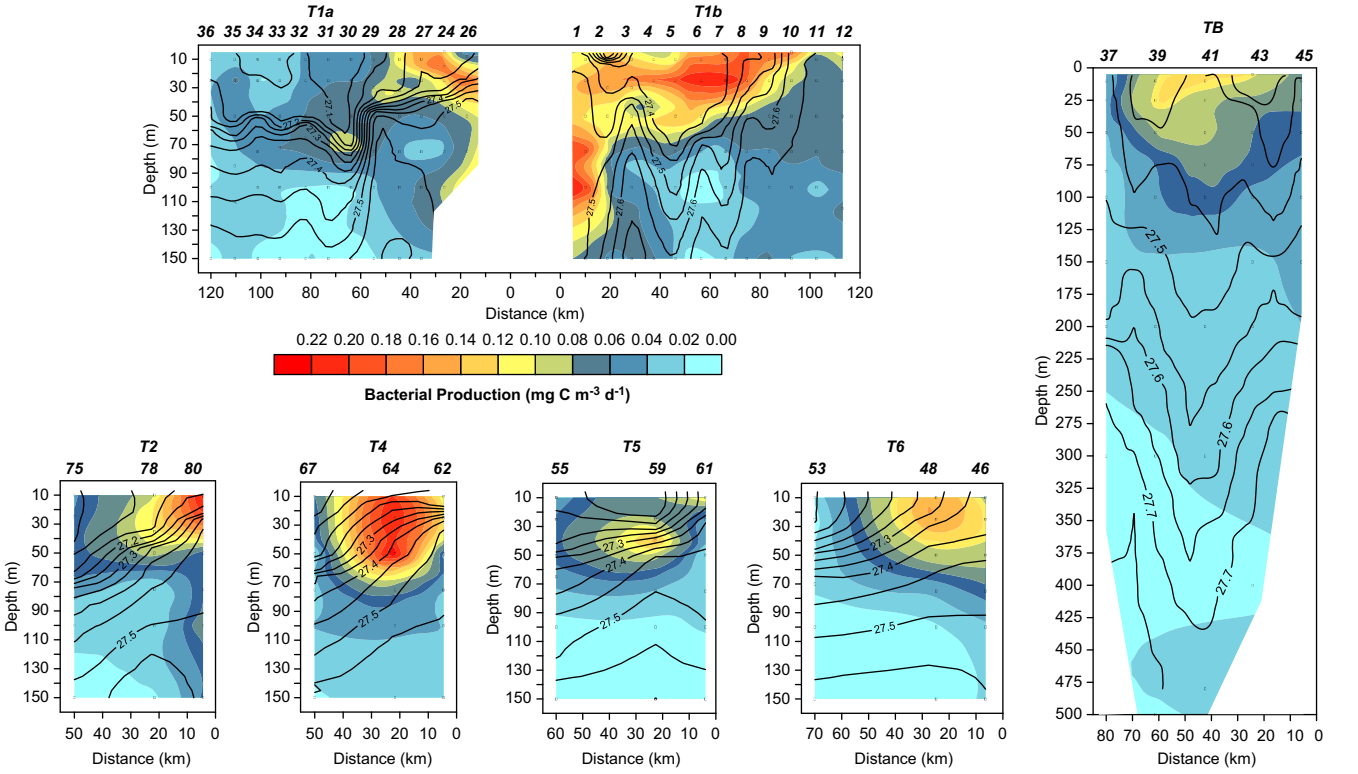

Fig. 8. Vertical distribution of bacterial production (mg C m^{-3} d^{-1}) along the transects sampled during the COUPLING cruise. Black superimposed isolines represent sigma-t. Numbers in the upper *X*-axis represent the station numbers.

Hewes, 2004; Corzo et al., 2005; Hewes, 2009). The limited contribution of microphytoplankton to total chlorophyll-a concentration has been previously associated to size-selective krill grazing over large-sized phytoplankton (Kawaguchi et al., 2001; Hewes, 2009). The increase of large-sized cells' contribution to phytoplankton biomass could indicate a non-selective grazing by salps, as hypothesized by Hewes (2009). Both surface and integrated chla concentration were very low in the northern part of

Table 2
Pearson correlation matrix among physical, chemical and biological variables. Correlations > 0.4 are marked in bold. Nonsignificant correlations (ns) are marked in italics.

N=192–257	Temp	Ammonia	Nitrate	Phosphate	Chla	FDOM-T
BP	0.260**	0.200**	−0.278**	−0.361**	**0.659****	**0.413****
Temp		0.180**	−0.353**	−0.332**	0.278**	*0.050 ns*
Ammonia			*−0.024* ns	−0.328**	*−0.092 ns*	*−0.032 ns*
Nitrate				0.336**	−0.164*	*−0.033 ns*
Phosphate					−0.147*	−0.179**
Chla						**0.416****

* $p < 0.05$.
** $p < 0.01$ (bilateral).

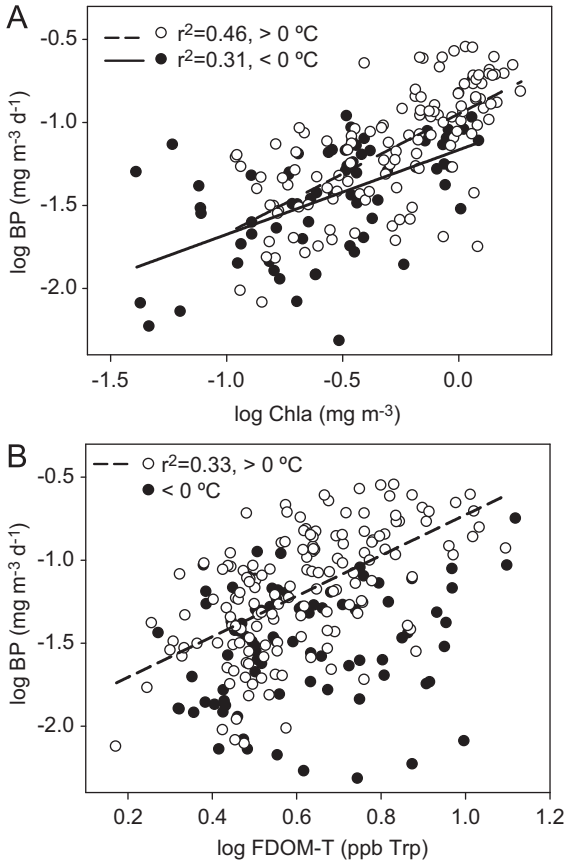

Fig. 9. Log–log relationship between (A) bacterial production (BP) and total chlorophyll-a concentration (chla) and (B) between bacterial production (BP) and protein-like fluorescence of dissolved organic matter (FDOM-T) at temperatures above (white symbols) or below (black symbols) 0 °C.

Drake Passage, where a DCM developed (Figs. 4 and 6A). Such low phytoplankton biomass levels and the formation of a DCM have been attributed to iron limitation (Holm-Hansen and Hewes, 2004; Hewes et al., 2009). Macronutrient concentrations in the upper 100 m of the water column were high enough to support high levels of phytoplankton biomass (nitrate > 18 μM, phosphate > 1.5 μM, silicate > 26 μM). Unfortunately, we do not have information about micronutrient concentrations, such as Fe. However, low iron concentrations (0.16–0.35 nM) have been previously measured in offshore Drake Passage waters (Martin et al., 1990; Hewes et al., 2008; Ardelan et al., 2010), whereas higher iron concentrations (1.9–3.1 nM) have been reported within the Bransfield Strait and in shelf waters around SSI (Hewes et al., 2008). The integrated Si* value, which has been proposed as an indicator for the degree of iron limitation (Sarmiento et al., 2003), explained 55% of the observed variability of integrated chla concentration (n=42), which supports the potential role of iron as the controlling factor of phytoplankton biomass distribution in the sampling area. Interestingly, when stations 3 and 4, characterized by relatively low chla concentrations and high Si*, and station 8, characterized by high chla concentrations and low Si* (Figs. 3B and 6A), were excluded from the analysis, the Si* tracer explained as much as 73% of integrated chla concentration variability (n=39). The low levels of phytoplankton biomass measured at stations 3 and 4 were not apparently explained by potential iron limitation, as they were characterized by high Si* values. These two stations were located in the southern edge of the Bransfield front (Fig. 1), defined by the steeply tilted isopycnals centered at station 2 (Fig. 4) (Sangrá et al., 2011). The low levels of phytoplankton biomass at these stations could be related to a strong grazing pressure in this frontal area. In support of this hypothesis, Hernández-León et al. (2000) and Vázquez et al. (2007) found the highest concentration of zooplankton and meroplankton biomass, respectively, associated to the Brandsfield front in the Brandsfield Strait during austral summer. On the other hand, the high levels of biomass at station 8 associated to low Si* levels could be related to an accumulation of phytoplankton biomass and the associated nutrient depletion. The relatively low primary production rates measured at this station (Table 1), in spite of the high chla concentration, support this hypothesis. Basterretxea and Arístegui (1999) also suggested that the advection of phytoplankton-rich waters generated in the nearby Bellingshausen Sea could in part explain the patchy distribution of chlorophyll-a in the Brandsfield Strait.

Primary production rates were relatively low (Table 1), particularly in the Drake Passage area, and within the range of volumetric rates previously measured in the area using the ^{14}C method (Burkholder and Mandelli, 1965; Arístegui et al., 1996; Kelley et al., 1999; Morán et al., 2001; Varela et al., 2002). The corresponding assimilation numbers were low, but within the range of previously reported values in the region (Burkholder and

Table 3
Measurements of bacterial respiration (BR), in situ bacterial production (unfiltered sample, $BP_{in\ situ}$) and time zero bacterial production (1.2 μm-filtered sample, BP_{T0}). Bacterial growth efficiency was estimated using BPT0. Temp, temperature; Chla, chlorophyll-a concentration; FDOM-T, protein-like fluorescence of dissolved organic matter. ND, not determined.

Stn	Depth (m)	BR (mg C m^{-3} d^{-1})	$BP_{in\ situ}$ (mg C m^{-3} d^{-1})	BP_{T0} (mg C m^{-3} d^{-1})	BGE (%)	Temp (°C)	Chla (mg m^{-3})	FDOM-T ppb Trp
64	5	4.03	ND	0.125	3.01	1.33	0.86	ND
64	100	3.46	0.043	0.043	1.23	0.15	0.34	3.53
72	45	2.78	0.084	0.218	7.27	1.13	1.15	4.35
72	100	2.98	0.085	0.120	3.87	0.01	0.22	2.99
78	35	5.76	0.140	0.503	8.03	0.93	0.69	4.31
78	100	4.51	0.020	0.028	0.62	−0.29	0.21	2.26

Mandelli, 1965; Basterretxea and Arístegui, 1999; Kelley et al., 1999; Morán et al., 2001; Lorenzo et al., 2002). Both the distribution and the range of mean water-column F_v/F_m (Fig. 3C) were in agreement with the previously reported values measured in the region (Hopkinson et al., 2007). The fact that 63% of the variability in F_v/F_m was explained by increases in the background relative fluorescence strongly suggests that low fluorescence yields could result from the synthesis of photosynthetic antennae complexes in excess under iron-deplete nitrogen-replete conditions (Schrader et al., 2011). The Si* tracer largely explained the observed variability in both primary production rates and F_v/F_m values, which suggest that phytoplankton activity in the area is potentially controlled by iron availability. The role of iron as a limiting factor for phytoplankton has been experimentally demonstrated in the region (Helbling et al., 1991; Hopkinson et al., 2007). Hopkinson et al. (2007) found a clear relationship between initial F_v/F_m values and the phytoplankton positive response to iron addition and concluded that F_v/F_m could be used to infer iron stress in this polar ecosystem.

Vertical stability of the water column has been proposed as a major mechanism controlling primary production in the Antarctic Ocean through light-limitation in well-mixed surface waters (e.g. Mitchell and Holm-Hansen, 1991). According to this hypothesis, a negative relationship would be expected between primary production rates and the upper mixed layer depth. The positive and significant relationship found in our dataset appears to be mainly related to the inclusion of station 10, located in the southern edge of the Peninsula Front, and characterized by the presence of nutrient-rich TWW. At this station, according to the chosen criteria (see Section 2) UML was very deep (134 m) and PP rates were maximal. Vernet et al. (2008) also showed that primary production positively correlates with mixed layer depth in coastal and slope waters in the west of Antarctic Peninsula. According to these authors, when phytoplankton biomass is very high, a deepening of the mixed layer may reduce light limitation. When we exclude station 10 from the analysis, there was no significant relationship between PP and UML depth, as previously observed in the Brandsfield Strait (Basterretxea and Arístegui, 1999). Several studies based on photosynthesis–irradiance experiments in the area concluded that overall light is not limiting phytoplankton primary production in this area during the austral summer (e.g. Figueiras et al., 1999; Lorenzo et al., 2002).

4.2. Bacterial metabolism and coupling with phytoplankton

Volumetric and integrated bacterial production rates were in the lower range of most papers published in the area during the same sampling period (Bird and Karl, 1999; Ortega-Retuerta et al., 2008; Manganelli et al., 2009), but similar to those reported by Kelley et al. (1999), Morán et al. (2001) and Pedrós-Alió et al. (2002). It is important to note that such differences with previous reports may in part reflect regional and interannual variability associated to variations in duration and extent of sea ice cover (Ducklow et al., 2012). In addition, most of the previous studies in the area assumed theoretical leucine to carbon conversion factors of 1.5 Kg C mol Leu^{-1} (Ortega-Retuerta et al., 2008) or 3.1 Kg C mol Leu^{-1} (Kelley et al., 1999; Morán et al., 2001; Manganelli et al., 2009), which are remarkably higher than the experimentally derived one by Pedrós-Alió et al. (2002) (0.81 Kg C mol Leu^{-1}) or our empirically derived conversion factor (0.74 Kg C mol Leu^{-1}). Among the multiple explanations posed for the low bacterial activity commonly reported in the polar seas, the simple control by dissolved organic matter (DOM) availability appears to be the most plausible (see review by Kirchman et al., 2009) which confronts with the traditional temperature–DOM control hypothesis by Pomeroy and co-workers (Pomeroy and Deibel, 1986; Pomeroy and Wiebe, 2001).

Multiple regression analysis revealed that BP variability in our dataset was best explained by chlorophyll-a concentration, FDOM-T and temperature, which suggest a dual control of temperature and substrate availability on bacterial activity. Similarly, Bird and Karl (1999) also found that both chlorophyll-a and temperature were important factors in predicting bacterial production in the Gerlache Strait. Pedrós-Alió et al. (2002) experimentally demonstrated that BP in western Antarctic waters increase with increasing temperature from −2 to 4 °C. On the other hand, a regional and decadal study by Ducklow et al. (2012) showed that temperature appears to influence, positively or negatively, BP in some regions or years but not in others. A negative relationship between BP and temperature may occur if there is a high accumulation of chla in the coldest waters. Kirchman et al. (2009) suggested that bacterial activity seems not to be more sensitive to temperature when DOM levels are low, as it would be predicted by the temperature–DOM hypothesis (Pomeroy and Wiebe, 2001). We found that bacterial activity seems to be more sensitive to temperature when substrate supply is high (Fig. 9). Simon and Rosenstock (2007) showed that dissolved protein was the major substrate for heterotrophic picoplankton growth in the Southern Ocean. Therefore, we used chla concentration as a proxy for substrate supply and the protein-like fluorescence of DOM as proxy for labile DOM supply. When chla or FDOM-T are low, the BP rates are similarly low irrespective of seawater temperature, whereas at high levels of chla or FDOMT, BP is consistently higher at temperatures above 0 °C (range 0.001–1.76 °C) than below 0 °C (range −1.05 to −0.01 °C). Indeed, there is no relationship between BP and FDOM-T at temperatures below 0 °C, and BP remains similarly low regardless of important increases in labile DOM supply. Thus, our dataset reveals a dual temperature–DOM control on bacterial production. When organic substrates are in short supply, temperature does not play a relevant role in controlling bacterial production rates, and thus, DOM availability appears to be the primary limiting factor. By contrast, when organic substrate concentration is higher, temperature appears to modulate the BP levels in these cold waters. The temperature effect on bacterial activity also appears evident when comparing chlorophyll-a concentration and integrated BP rates (Fig. 6A and B). A major disconnection between both components occurs at stations 11–12, where integrated chlorophyll-a is very high and integrated BP rates are very low, which is likely explained by the very low mean seawater temperatures (−0.78 °C) at these stations (Fig. 3A). Nevertheless, the great data dispersion in Fig. 9 plots, as well as the low percentage of variability explained by chla concentration, FDOM-T and temperature (53%), clearly indicates that other factors, such as grazing pressure or viral lysis, must also play a role in regulating bacterial dynamics in this area (Bird and Karl, 1999; Pedrós-Alió et al., 2002).

Bacterial production represented on average only 3.9% of co-occurring primary production (range 0.5–15%), which is within the range of values reported in the previous studies in the Antarctic ecosystems (1–20%) (Bird and Karl, 1999; Ducklow et al., 2001; Morán et al., 2001; Pedrós-Alió et al., 2002; Kirchman et al., 2009; Ducklow et al., 2012). The low fraction of primary production processed by bacteria in the polar oceans has been traditionally interpreted as a fundamental uncoupling between autotrophic and heterotrophic compartments in perennially cold waters (e.g. Karl, 1993; Bird and Karl, 1999). However, other evidences, such as significant correlations between BP and dissolved primary production rates or chlorophyll-a concentration, suggest that both components of the microbial plankton community are as coupled as they are in other warmer oceans not affected by allochthonous inputs (Morán et al., 2001; Ortega-Retuerta et al., 2008; Ducklow et al., 2012). Similarly, despite the low contribution of our BP estimates to

PP, we also did find a significant correlation between BP and chlorophyll-a concentration (Table 2, Fig. 9), which suggests a relatively important link between bacteria and phytoplankton in the sampling area during the austral summer.

It has been also suggested that the apparent uncoupling between phytoplankton and bacteria in the Antarctic waters could partially derive from the non-inclusion of mesopelagic bacterial activity, given the high rates of export production typical of these cold pelagic ecosystems (Ducklow et al., 2001; Simon et al., 2004). Simon et al. (2004) estimated that epi- and mesopelagic bacterial production accounted for 20% of the total primary production in the Antarctic polar frontal region. Similarly, the integrated BP measured in transect TB was 72% higher when integrating down to 300–500 m than when integrating down to 100 m.

Additionally, to adequately assess the prokaryotic consumption of PP, it is important to consider the fraction of PP which is utilized for bacterial respiration. There are no direct estimates of bacterial respiration in this area, although Arístegui et al. (1996) and Serret et al. (2001) did reported high rates of microbial community respiration (from 2.9 to ca. 90 mg C m^{-3} d^{-1}) in the Brandsfield Strait. Our bacterial respiration rates were all below or in the low end of the range for total community respiration. Carlson et al. (1999) directly estimated bacterial respiration and bacterial growth efficiency using long-term (15 days) incubations of 0.8 μm filtrated seawater in the surface water of the Ross Sea during summer. The derived BGE values ranged from 9% to 38%, which are considerably higher than our estimates (0.6–8%) based on relatively short incubations (3 days). The BGE was positively correlated with temperature ($r^2=0.42$), chlorophyll-a ($r^2=0.46$), and FDOM-T ($r^2=0.71$), but not with inorganic nutrients, which further points to DOM availability as the major controlling factor of bacterial growth. The lower BGE estimates, as compared to the Ross Sea, may simply reflect differences in ecosystem productivity, in fact, the concentration of chlorophyll-a in the Ross Sea ranged from 3.1 to 8.6 mg m^{-3} (Carlson et al., 1999), whilst chla concentration in our samples ranged from 0.21 to 1.15 mg m^{-3} (Table 3). Using a mean BGE of 6.1% for the upper mixed layer, the bacterial carbon demand (bacterial production plus bacterial respiration) would account, on average, for 63% of the total primary production, which is similar to the percentages frequently found in warmer relatively productive waters (Teira et al., 2003; Reinthaler and Herndl, 2005; Alonso-Sáez et al., 2007; Sintes et al., 2010).

In conclusion, we have found that whereas phytoplankton seems to be controlled by iron availability, bacterial metabolism appears to be primarily controlled by organic carbon supply and by water temperature, when substrate levels are high. Moreover, the fraction of primary production consumed by bacteria was comparable to that in the temperate waters, which strongly supports that the coupling between the autotrophic and heterotrophic components does appear to be similar in this polar area than in other oceanic regions.

Acknowledgments

We thank all the people involved in the COUPLING project who helped with the cruise preparation and sampling. We are grateful to L. Lubián, C. García and C. García-Muñoz for nutrient sampling, X.A. Álvarez-Salgado for advice and help with fluorescence analyses, and P. Sangrá for oceanographic data. We also thank the officers and crew of the R/V Hespérides, as well as the staff of the Technical Support Unit (UTM), for their support during the work at sea.

This research was supported by the MICINN contracts COUPLING (CTM2008-06343-C02-02) and DIFUNCAR (CTM2008-03790). S.M.-G. was funded by a F.P.U. MEC fellowship. C.S. was funded by a Parga y Pondal-Xunta de Galicia contract. E.T. and B.M.-C. were funded by a Ramón y Cajal-MEC contract.

References

Alonso-Sáez, L., Vázquez-Dominguez, E., Cardelus, C., et al., 2007. Factors controlling the year-round variability in carbon flux through bacteria in a coastal marine system. Ecosystems 11, 397–409.

Ardelan, M.V., Holm-Hansen, O., Hewes, C.D., Reiss, C.S., Silva, N.S., Dulaiova, H., Steinnes, E., Sakshaug, E., 2010. Natural iron enrichment around the Antarctic Peninsula in the Southern Ocean. Biogeosciences 7, 11–25.

Arístegui, J., Montero, M.F., Ballesteros, S., Basterretxea, G., van Lenning, K., 1996. Planktonic primary production and microbial respiration measured by ^{14}C assimilation and dissolved oxygen changes in coastal waters of the Antarctic Peninsula during austral summer: implications for carbon flux studies. Mar. Ecol. Prog. Ser. 132, 191–201.

Azam, F., 1998. Microbial control of oceanic carbon flux: the plot thickens. Science 280, 694–696.

Basterretxea, G., Arístegui, J., 1999. Phytoplankton biomass and production during late austral spring (1991) and summer (1993) in the Bransfield Strait. Polar Biol. 21, 11–22.

Billen, G., Becquevort, S., 1991. Phytoplankton–bacteria relationship in the Antarctic marine ecosystem. Polar Res. 10, 245–253.

Bird, D.F., Karl, D.M., 1999. Uncoupling of bacteria and phytoplankton during the austral spring bloom in Gerlache Strait, Antarctic Peninsula. Aquat. Microb. Ecol. 19, 13–27.

Bjørnsen, P.K., Kuparinen, J., 1991. Determination of bacterioplankton biomass, net production and growth efficiency in the Southern Ocean. Mar. Ecol. Prog. Ser. 71, 185–194.

Burkholder, P.R., Sieburth, J.M., 1961. Phytoplankton and chlorophyll in the Gerlache and Bransfield Straits of Antarctica. Limnol. Oceanogr. 6, 45–52.

Burkholder, P.R., Mandelli, E.F., 1965. Carbon assimilation of marine phytoplankton in Antarctica. Proc. Natl. Acad. Sci. 54, 437–444.

Calvo-Díaz, A., Morán, X.A.G., 2009. Empirical leucine-to-carbon conversion factors for estimating heterotrophic bacterial production: seasonality and predictability in a temperate coastal ecosystem. Appl. Environ. Microbiol. 75, 3216–3221.

Carlson, C.A., Bates, N.R., Ducklow, H.W., Hansell, D.A., 1999. Estimation of bacterial respiration and growth efficiency in the Ross Sea, Antarctica. Aquat. Microb. Ecol. 19, 229–244.

Corzo, A., Rodríguez-Gálvez, S., Lubián, L., Sobrino, C., Sangrá, P., Martínez, A., 2005. Antarctic marine bacterioplankton subpopulations discriminated by their apparent content of nucleic acids differ in their response to ecological factors. Polar Biol. 29, 27–39.

Duarte, C.M., Agustí, S., Vaqué, D., Agawin, N.S.R., Felipe, J., Casamayor, E.O., Gasol, J.M., 2005. Experimental test of bacteria–phytoplankton coupling in the Southern Ocean. Limnol. Oceanogr. 50, 1844–1854.

Ducklow, H.W., 2000. Bacterioplankton production and biomass in the oceans. In: Kirchman, D.L. (Ed.), Microbial Ecology of the Oceans. Wiley, New York, pp. 85–120.

Ducklow, H.W., Carlson, C.A., Church, M., Kirchman, D., Smith, D., Steward, G., 2001. The seasonal development of the bacterioplankton bloom in the Ross Sea, Antarctica, 1994–1997. Deep-Sea Res. II 48, 4199–4221.

Ducklow, H.W., Baker, K., Martinson, D.G., et al., 6, 2007. Marine pelagic ecosystems: the West Antarctic Ecosystem. Philos. Trans. R. Soc. B 362, 67–94.

Ducklow, H.W., Schofield, O., Vernet, M., Stammerjohn, S., Erickson, M., 2012. Multiscale control of bacterial production by phytoplankton dynamics and sea ice along the western Antarctic Peninsula: a regional and decadal investigation. J. Mar. Syst. 98–99, 26–39.

García, M.A., López, O., Sospedra, J., Espino, M., Gracia, V., Morrison, G., Rojas, P., Figa, J., Puigdefàbregas, J.S., Arcilla, A., 1994. Mesoscale variability in the Brandsfield Strait region (Antarctica) during austral summer. Ann. Geophys. 12, 856–867.

Hansen, H.P., Grasshoff, K., 1983. Automated chemical analysis. In: Grasshoff, K., Ehrhardt, M., Krernling, K. (Eds.), Methods of Seawater Analysis. Verlag Chemie, Weinheim, pp. 347–379.

Hama, T., Miyazaki, T., Ogawa, Y., Iwakuma, T., Takahashi, M., Otsuki, A., Ichimura, S., 1983. Measurement of photosynthetic production of a marine phytoplankton population using a stable ^{13}C isotope. Mar. Biol. 73, 31–36.

Helbling, E.W., Villafañe, V., Holm-Hansen, O., 1991. Effect of iron on productivity and size distribution of Antarctic phytoplankton. Limnol. Oceanogr. 36, 1879–1885.

Hernández-León, S., Almeida, C., Portillo-Hahnefeld, A., Gómez, M., Montero, I., 2000. Biomass and potential feeding, respiration and growth of zooplankton in the Bransfield Strait (Antarctic Peninsula) during austral summer. Polar Biol. 23, 679–690.

Hewes, C.D., Reiss, C.S., Kahru, M., Mitchell, B.G., Holm-Hansen, O., 2008. Control of phytoplankton biomass by dilution and mixing depth in the western Weddell-Scotia Confluence. Mar. Ecol. Prog. Ser. 366, 15–29.

Hewes, C.D., Reiss, C.S., Holm-Hansen, O., 2009. A quantitative analysis of sources for summertime phytoplankton variability over 18 years in the South Shetland Islands (Antarctica) region. Deep-Sea Res. I 56, 1230–1241.

Hewes, C.D., 2009. Cell size of Antarctic phytoplankton as a biogeochemical condition. Antarct. Sci. 21, 470–547.

Holm-Hansen, O., Amos, A.F., Silva, N.S., Villafañe, V., Helbling, E.W., 1994. In situ evidence for a nutriente limitation of phytoplankton growth in pelagic Antarctic Waters. Antarct. Sci. 6, 315–324.
Holm-Hansen, O., Hewes, C.D., 2004. Deep chlorophyll-a maxima (DCMs) in Antarctic waters: I relationships between DCMs and the physical, chemical, and optical conditions in the upper water column. Polar Biol. 27, 699–710.
Hopkinson, B.M., Mitchell, B.G., Reynolds, R.A., et al., 2007. Iron limitation across chlorophyll gradients in the southern Drake Passage: phytoplankton responses to iron addition and photosynthetic indicators of iron stress. Limnol. Oceanogr. 52, 2540–2554.
Figueiras, F.G., Arbones, B., Estrada, M., 1999. Implications of bio-optical modeling of phytoplankton photosynthesis in Antarctic waters: further evidence of no light limitation in the Brandsfield Strait. Limnol. Oceanogr. 44, 1599–1608.
Karl, D.M., Holm-Hansen, O., Taylor, G.T., Tien, G., Bird, D.F., 1991. Microbial biomass and productivity in the western Bransfield Strait, Antarctica during the 1986–87 austral summer. Deep-Sea Res. 38, 1029–1055.
Karl, D.M., 1993. Microbial processes in the Southern Oceans. In: Friedmann, E.I. (Ed.), Antarctic Microbiology. Wiley, New York, pp. 1–63.
Kawaguchi, S., Shiomoto, A., Imai, K., Tsarina, Y., Yamaguchi, H., Noiri, Y., Iguchi, N., Kameda, T., 2001. A possible explanation for the dominance of chlorophyll in pico and nano-size fractions in the waters around the South Shetland Islands. Ocean Polar Res. 23, 379–388.
Kelley, C.A., Pakulski, J.D., Sandvik, S.L.H., Coffin, R.B., Downer, R.B., Aas, P., Lyons, M.M., Jeffrey, W.H., 1999. Phytoplanktonic and bacterial carbon pools and productivities in the Gerlache Strait, Antarctica, during early austral spring. Microb. Ecol. 38, 296–305.
Kirchman, D.L., Morán, X.A.G., Ducklow, H., 2009. Microbial growth in the polar oceans—role of temperature and potential impact of climate change. Nat. Rev. Microbiol. 7, 451–459.
Lorenzo, L.M., Arbones, B., Figueiras, F.G., Tilstone, G.H., Figueroa, F.L., 2002. Photosynthesis, primary production and phytoplankton growth rates in Gerlache and Bransfield Straits during austral summer: cruise FRUELA 95. Deep-Sea Res. II 49, 707–721.
Manganelli, M., Malfatti, F., Samo, T.J., Mitchell, B.G., Wang, H., Azam, F., 2009. Major role of microbes in carbon fluxes during austral winter in the southern Drake Passage. Plos One 4, e6941.
Martin, J.H., Gordon, R.M., Fitzwater, S.E., 1990. Iron in Antarctic waters. Nature 345, 156–158.
Mitchell, B.G., Holm-Hansen, O., 1991. Observations and modeling of the Antarctic phytoplankton crop in relation to mixing depth. Deep-Sea Res. 38, 981–1007.
Morán, X.A.G., Gasol, J.M., Pedrós-Alió, C., Estrada, M., 2001. Dissolved and particulate primary production and bacterial production in offshore Antarctic waters during austral summer: coupled or uncoupled? Mar. Ecol. Prog. Ser. 222, 25–39.
Mourino-Carballido, B., McGillicuddy, D.J., 2006. Mesoscale variability in the metabolic balance of the Sargasso Sea. Limnol. Oceanogr. 51, 2675–2689.
Mullins, B.W., Priddle, J., 1987. Relationships between bacteria and phytoplankton in the Bransfield Strait and southern Drake Passage. Br. Antarct. Surv. Bull. 76, 51–64.
Neale, P.J., Sobrino, C., Gargett, A.E., 2012. Vertical mixing and the effects of solar radiation on photosystem II electron transport by phytoplankton in the Ross Sea Polynya. Deep Sea Res. I (63), 118–132.
Nieto-Cid, M., Álvarez-Salgado, X.A., Pérez, F.F., 2005. DOM fluorescence, a tracer for biogeochemical processes in a coastal upwelling system (NW Iberian Peninsula). Mar. Ecol. Prog. Ser. 297, 33–50.
Ortega-Retuerta, E., Reche, I., Pulido-Villena, E., Agustí, S., Duarte, C.M., 2008. Exploring the relationship between active bacterioplankton and phytoplankton in the Southern Ocean. Aquat. Microb. Ecol. 52, 99–106.
Pedrós-Alió, C., Vaqué, D., Guixa-Boixereu, N., Gasol, J.M., 2002. Prokaryotic plankton biomass and heterotrophic production in western Antarctic waters during 1995–1996 austral summer. Deep-Sea Res. II 49, 805–825.
Pomeroy, L.R., Deibel, D., 1986. Temperature regulation of bacterial activity during the spring bloom in Newfoundland coastal waters. Science 233, 359–361.
Pomeroy, L.R., Wiebe, W.J., 2001. Temperature and substrates as interactive limiting factors for marine heterotrophic bacteria. Aquat. Microb. Ecol. 23, 187–204.
Reinthaler, T., Herndl, G.J., 2005. Seasonal dynamics of bacterial growth efficiencies in relation to phytoplankton in the southern North Sea. Aquat. Microb. Ecol. 39, 7–16.
Robinson, C., 2008. Heterotrophic bacterial respiration. In: Kirchman, D.L. (Ed.), Microbial Ecology of the Oceans, 2nd edition Wiley-Liss, New York, pp. 299–336.
Sangrá, P., Gordo, C., Hernández-Arencibia, M., Marrero-Díaz, A., Rodríguez-Santana, A., Stegner, A., Martínez-Marrero, A., Pelegrí, J.L., Pichon, T., 2011. The Bransfield current system. Deep-Sea Res. I 58, 390–402.
Sarmiento, J.L., Le Quéré, C., 1996. Oceanic carbon dioxide uptake in a model of century-scale global warming. Science 274, 1346–1350.
Sarmiento, J.L., Gruber, N., Brzezinski, M.A., Dunne, J.P., 2003. High-latitude controls of thermoclines nutrients and low latitude biological productivity. Nature 427, 56–60.
Schrader, P.S., Milligan, A.J., Behrenfeld, M.J., 2011. Surplus photosynthetic antennae complexes underlie diagnostics of iron limitation in a cyanobacterium. Plos One 6, e18753.
Serret, P., Fernández, E., Anadón, R., Varela, M., 2001. Trophic control of biogenic carbon export in Bransfield and Gerlache straits, Antarctica. J. Plankton Res. 23, 1345–1360.
Simon, M., Rosenstock, B., Zwisler, W., 2004. Coupling of epipelagic and mesopelagic heterotrophic picoplankton production to phytoplankton biomass in the Antarctic polar frontal region. Limnol. Oceanogr. 49, 1035–1043.
Simon, M., Rosenstock, B., 2007. Different coupling of dissolved amino acid, protein, and carbohydrate turnover to heterotrophic picoplankton production in the Southern Ocean in asutral summer and fall. Limnol. Oceanogr. 52, 58–95.
Sintes, E., Stoderegger, K., Parada, V., Herndl, G.J., 2010. Seasonal dynamics of dissolved organic matter and microbial activity in the coastal North Sea. Aquat. Microb. Ecol. 60, 85–95.
Smith, D.C., Azam, F., 1992. A simple, economical method for measuring bacterial protein synthesis rates in seawater using 3H-leucine. Mar. Microb. Food Webs 6, 107–114.
Teira, E., Abalde, J., Álvarez-Ossorio, M.T., et al., 2003. Plankton carbon budget in a coastal wind-driven upwelling station off A Coruña (NW Iberian Peninsula). Mar. Ecol. Prog. Ser. 265, 31–43.
Varela, M., Fernández, E., Serret, P., 2002. Size-fractionated phytoplankton biomass and primary production in the Gerlache and south Bransfield Straits (Antarctic Peninsula) in austral summer 1995–1996. Deep-Sea Res. II 49, 749–768.
Vázquez, E., Ameneiro, J., Putzeys, S., Gordo, C., Sangrá, P., 2007. Distribution of meroplankton communities in the Bransfield Strait, Antarctica. Mar. Ecol. Prog. Ser. 338, 119–129.
Vernet, M., Martinson, D., Iannuzzi, R., Stammerjohn, S., Kozlowski, W., Sines, K., Smith, R., Garibotti, I., 2008. Primary production within the sea-ice zone west of the Antarctic Peninsula: I—sea ice, summer mixed layer, and irradiance. Deep-Sea Res. II 55, 2068–2085.
Williams, P.J.leB., del Giorgio, P.A., 2005. Respiration in aquatic ecosystems: history and background. In: del Giorgio, P.A., Williams, P.J.leB (Eds.), Respiration in Aquatic Ecosystems. Oxford University Press, London, pp. 1–18.